ARTICLES

Electron states in a nearly ideal random-network model of amorphous SiO_2 glass

Ming-Zhu Huang and W. Y. Ching
Department of Physics, University of Missouri–Kansas City, Kansas City, Missouri 64110
(Received 29 December 1995; revised manuscript received 28 March 1996)

A large continuous random-network model with 1296 atoms and periodic boundary conditions has been constructed for amorphous SiO_2 glass. The atoms in this model are all fully coordinated with an overall small bond length and bond angle distortions. The calculated pair distribution function is in close agreement with the diffraction data. Based on this model, a first-principles calculation of the electron states is performed and the resulting wave functions are analyzed. Subtle differences in the density of states with the crystalline SiO_2 are found. The calculated density of states are in good agreement with x-ray emission data and show the importance of Si $3d$ orbitals. The distributions of effective charges on Si and O atoms are studied in relation to the short-range order in the glass. It is found that O atoms with a Si-O-Si bridging angle of less than 120° have smaller effective charges and can be identified as quasidefective centers that are responsible for the two-level tunneling at low temperature. It is also shown that localized states at the top of the band are induced by the elongation of the Si-O bond and those at the bottom of the band are related to atoms with shortened bonds. A mobility edge of 0.2 eV at the top of the valence band is obtained. A similar mobility edge for the conduction band cannot be located because of the much less localized nature of the states. [S0163-1829(96)01731-6]

I. INTRODUCTION

It has been well established[1] that the structure of amorphous SiO_2 (a-SiO_2) glass is best described by the continuous random-network (CRN) model in which the Si atom is tetrahedrally bonded to four O atoms and the O atom bridges between two Si atoms with a very flexible Si-O-Si bridging angle.[2,3] The CRN model for a-SiO_2 glass is therefore a paradigm for studying noncrystalline solids with well-defined short-range order (SRO), subtle intermediate-range order (IRO), and no long-range order (LRO). Over the years, there have been many attempts to construct CRN models[4–21] for a-SiO_2 and then use these models to study the electronic[22–25] and vibrational[18,24,26–29] properties of the glass. These models are in the form of either a large cluster with a free surface or a cubic box with periodic boundary conditions. The quality of the model is generally measured by the agreement between the pair distribution function (PDF) computed from the model and those obtained from diffraction techniques.[30–41] Another criterion is the degree of bond length (BL) and bond angle (BA) distortions from the ideal values. The periodic CRN models are more appealing because they represent a truly infinite array of atoms provided that the models are sufficiently large in size. However, imposing a periodic boundary condition on a covalently bonded network is not an easy task and such models generally end up having too large BL and BA distortions. In recent years, molecular-dynamics (MD) techniques have been quite popular in generating a-SiO_2 models using either pair-wise potentials[8–10,15,18] or using a first-principles approach of simulated annealing.[25] However, the MD technique generally involves movements of atoms at finite temperatures under a local force field. The quenched structure obtained as a snapshot of the simulation at low temperature usually has large distortions and always contains defective centers such as over- or undercoordination or broken bonds and therefore is not representative of a perfect CRN in which the topology of the network is precisely defined. Although the MD simulation may mimic the real structure in a glassy material at finite temperatures, for the purpose of studying the electron states in an ideal noncrystalline solid, it is better to have a near perfect CRN model free of major defects and large distortions such that the structure-properties relationship can be more transparent. Once a near-perfect CRN model is available, the effects of specific defects and large distortions can be studied in a more focused way by modifying the existing model.

In a covalent glass model for a-Si or a-SiO_2, the imposition of a periodic boundary condition implies an increased strain on the network, which should be reflected in the increased bond length and bond angle distortions. It is expected that the larger the model, the smaller the strain induced by the periodic boundary condition. This notion is partially supported by the fact that the earlier model with only 162 atoms[43] has a larger distortion than the present model of 1296 atoms. On the other hand, a cluster type of model with a free surface will have less strain since the atoms on the surface are not required to have the specific directional bonding as in the periodic model. However, the mass density of a cluster model cannot be precisely determined, and calculation of electron states based on a cluster model will have the calculated spectrum contaminated by the surface states, which will be quite difficult to separate from the bulk states.

Since the local bonding structure in a-SiO_2 is similar to its crystalline counterpart in α quartz and several other SiO_2

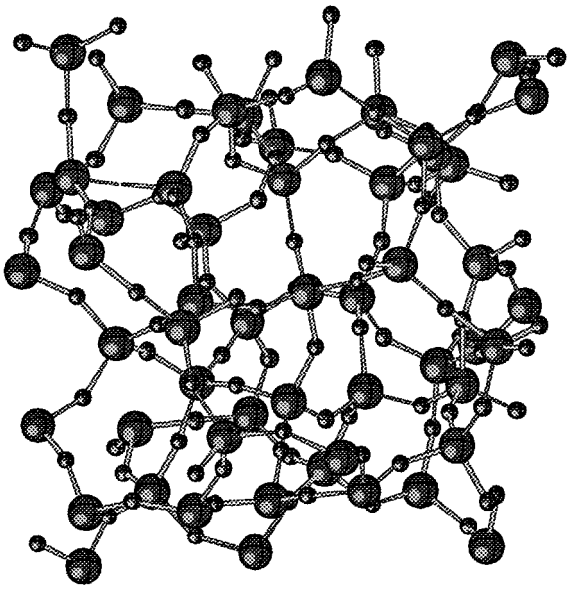

FIG. 1. Ball and stick sketch of a portion of a near-ideal model of a-SiO_2. Large circles are for Si and small circles for O. The entire model has 1296 atoms.

polymorphs,[42] it is reasonable to expect the electronic structure of the two to be similar. However, there are subtle differences that reflect the loss of LRO such as the localization of states near the band edges, the existence of mobility edges, and the distribution of effective charges. To understand the nature of electron states in a-SiO_2, first-principles calculations based on a near-perfect CRN model of sufficient size will be most desirable. In this paper, we report the results of such a calculation. In Sec. II the construction and the characteristics of a large CRN model for a-SiO_2 are described. This is followed, in Sec. III, by the description of the results and the analysis of the electron states in such a model. The identification of a few O atoms with Si-O-Si bridging angles less than 120° as quasidefective centers is emphasized and elaborated. Section IV is devoted to the discussion of these results and the tremendous potential of using such models in elucidating the structures and properties of other covalently bonded glasses, their composites, interfaces, and defects.

II. MODEL STRUCTURE

Figure 1 shows a ball-and-stick portrayal of a near-perfect CRN model for a-SiO_2. The model contains 432 SiO_2 molecules (1296 atoms) with periodic boundary conditions. It was generated from a smaller seed model studied by one of us 15 years ago.[43] The model is constrained to have the density of 2.23 g/cm^3 and relaxed by means of Monte Carlo steps using a Keating type of potential.[44] This density is slightly larger than the experimental density of 2.20 g/cm^3 for vitreous silica, which may contain small porous regions not found in an ideal CRN model. Because the model is fairly large and the local nearest-neighbor (NN) bonding for each atom is determined *a priori*, the constraint imposed by the periodic boundary condition is less stringent and the structure has reasonable BL and BA distortions. Each atom

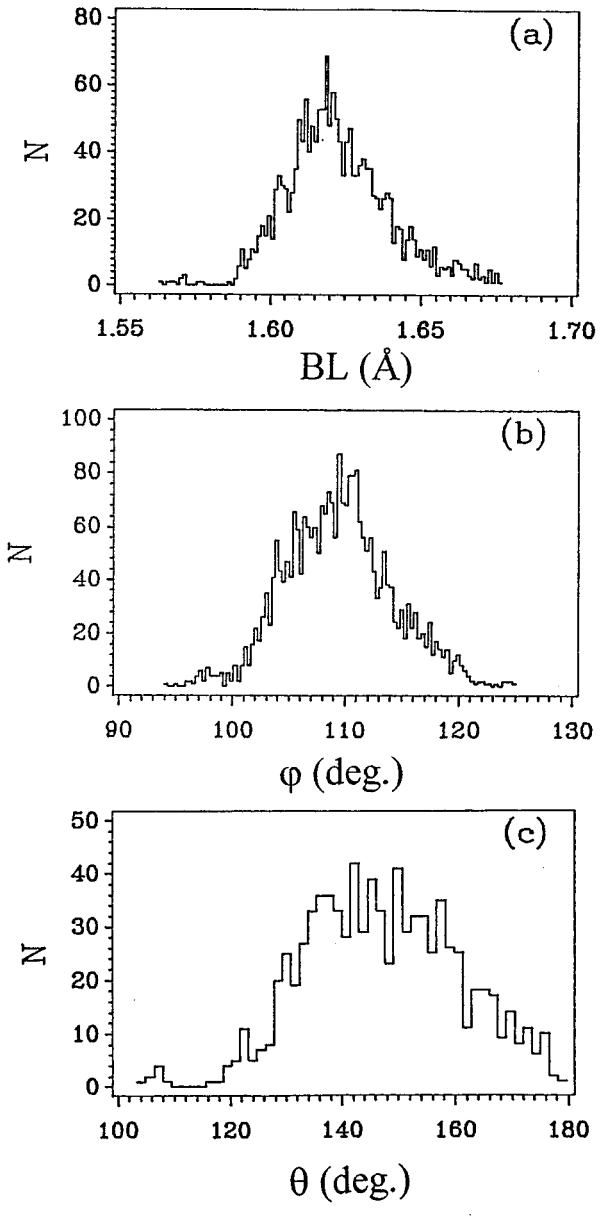

FIG. 2. Distributions of (a) Si-O bond lengths, (b) O-Si-O bond angles, and (c) Si-O-Si bridging angles in degrees.

is fully coordinated with no broken bonds. Figure 2 shows the distributions of the Si-O BL and the O-Si-O (φ) and Si-O-Si (θ) bond angles in this model. The distributions are close to a Gaussian form. The average Si-O BL is 1.622 Å, with a standard deviation of only 0.017 Å. The Si-centered tetrahedral units are well preserved since the average O-Si-O angle of 109.38° is very close to the tetrahedral angle of 109.47° and a standard deviation of 4.69°. The O bridging angles are much more flexible. The average Si-O-Si angle in our model is 147.06°, with a standard deviation of 13.52°. This average angle is very close to the experimentally measured most probable angle of 145° (Ref. 30) and the distribution shown in Fig. 2(c) is quite similar to that determined by Dupree and Pettifer using magic angle spinning NMR spectroscopy.[45] To have a better idea about the IRO of the model, the distributions of the Si-Si and O-O separations are shown in Fig. 3. From Figs. 2(c) and 3(a) it can be seen that

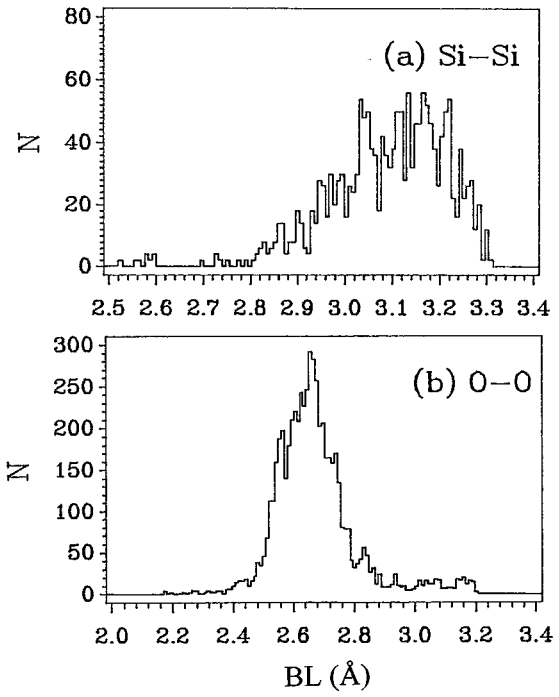

FIG. 3. Distributions of (a) Si-Si separations and (b) O-O separations.

there are a few O atoms with bridging angles less then 120° that also result in the Si-Si separations of less than 2.6 Å. These O atoms have special implications on the microscopic origin of tunneling centers in glasses and will be discussed in more detail in the following sections. The model does not contain any three-member or four-member rings, but contains a small percentage of five-member rings. (Here a ring is defined as a closed loop of either Si or O atoms.) It has been concluded by several authors that the distribution of the dihedral angles of the tetrahedral units are random and does not correlate with other parameters of the model.[1,19] Therefore, this is not investigated in the present model. The physical characteristics of the model are listed in Table I. Similar data for the Bell-Dean model[5] are also listed for comparison.

TABLE I. Physical characteristics of the CRN models for a-SiO_2.

Characteristic	Present model	Bell and Dean (Ref. 5)
Density	2.23 g/cm^3	1.99 g/cm^3
No. of atoms	1296	614 (interior of a cluster)
Cube size	26.958 Å	
Mean BL and deviation	1.622±0.017 Å	1.6±3.5%
Mean BA and deviation		
O-Si-O (θ)	109.38°±4.69°	109.3°±6%
Si-O-Si (φ)	147.06°±13.52°	153°±6%
Peak positions in the PDF (Å)		
$P1$	1.62 (Si-O)	
$P2$	2.60 (O-O)	
$P3$	3.11 (mainly Si-Si)	
$P4$	4.10 (Si-O, some Si-Si, and O-O)	
$P5$	4.97 (Si-Si, some O-O, and Si-O)	
$P6$	6.19 (Si-O, some Si-Si, and O-O)	

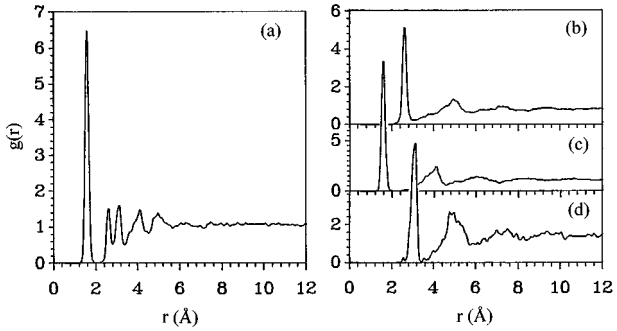

FIG. 4. (a) Calculated PDF $g(r)$ for a-SiO_2, (b) partial PDF of O-O, (c) partial PDF of Si-O, and (d) partial PDF of Si-Si (a) is obtained from (b)–(d) with different weighting factors for each partial component. See the text for details.

Figure 4 shows the calculated pair PDF $g(r)$ of the model and also its partial components. The total PDF is obtained from the partial components by appropriate weighting factors.[46] The PDF of the model is in general agreement with the existing diffraction data.[30–32,34,41] The small discrepancy is probably related to the presence of some O atoms with small Si-O-Si angles discussed above. Based on the calculated PDF, it can be concluded that the present model of a near-perfect CRN represents the structure of a-SiO_2 very well. The peak positions in the PDF and their atomic origins are also listed in Table I.

III. ELECTRON STATES

The real-space orthogonalized linear combination of atomic orbitals[47] (OLCAO) method is used to calculate the electron states in the CRN model of a-SiO_2. The OLCAO method has a unique advantage in that the solid-state wave functions are expanded in terms of atom-centered atomic orbitals and the potential is in the form of the sum of atom-centered atomiclike potentials. For systems with the same kind of chemical bonding, this type of atom-centered potential function is transferable. Accordingly, we used the self-consistent potential derived from the recent crystalline calculations in the local-density approximation (LDA) for α quartz (c-SiO_2) and the same basis functions as for all other polymorphs of SiO_2.[42] This approach is not as rigorous as the full self-consistent calculation of the 1296-atom model itself, which would be rather impractical, but is a significant improvement over the earlier calculations[22,48,49] using non-self-consistent potentials or potentials derived from a simpler charge self-consistent procedure.[24] It is at a much higher level of accuracy than the tight-binding approximation,[23] where the interaction parameters are only estimated and limited to NN or next-NN interactions. In the present approach, the Hamiltonian and the overlap matrix elements of the glass model are calculated exactly for interactions up to any NN atoms; thus the fine structural characteristics and the IRO of the model are fully reflected in the calculation. Since no arbitrary parameters are introduced and all the interaction integrals are calculated based on the transferable potential from α-SiO_2, the present study on a-SiO_2 can be considered

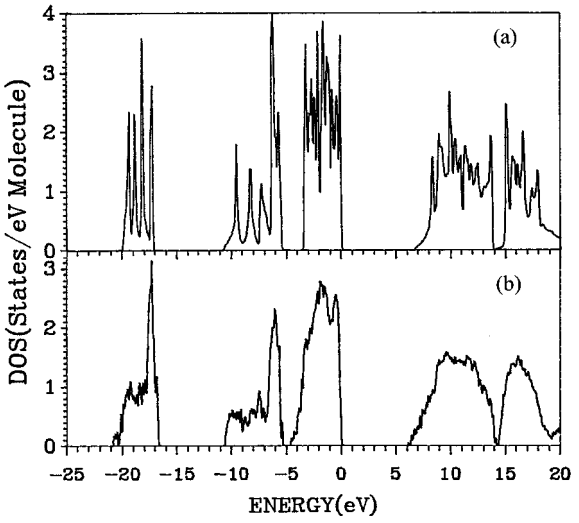

FIG. 5. Calculated total DOS of (a) α quartz and (b) a-SiO_2.

to be first principles in nature. In the present calculation, the basis functions consist of the Si $3s$, Si $3p$, Si $4s$, Si $3d$, O $2s$, and O $2p$ orbitals in addition to the core orbitals. The extra orbitals beyond the minimal basis set enable us to obtain the unoccupied states more accurately and also to account for the hybridization of the Si $3d$ states with the O $2p$ orbitals. With 432 Si atoms and 864 O atoms in the model and after the orthogonalization to the core procedure that eliminates the core states ($1s$,$2s$,$2p$ of Si and $1s$ of O), the final secular equation has a dimension of 7776×7776. For a large model such as the present one, a single diagonalization at $k=0$, where all the matrix elements are real, is more than sufficient.

A. Density of states

Figure 5 shows the calculated density of states (DOS) of the CRN model of a-SiO_2. Also shown for comparison is the corresponding result for α quartz with the same basis set. Although the general features of the DOS for the two are similar because of similarities in the SRO, there are substantial differences in fine structures that reflect the difference in the LRO and the IRO. Such fine differences in the electron DOS between a-SiO_2 and c-SiO_2 have seldom been discussed in the literature. Experimental data from x-ray photoelectron spectroscopy or x-ray emission spectroscopy do not have the sufficient resolution to resolve these differences. A common practice in the existing calculations for a-SiO_2 has been to broaden the DOS spectra, which masks these differences. For example, the O $2s$ band for c-SiO_2 at -17 to -20 eV has four well-resolved sharp peaks, while in a-SiO_2 there is only one sharp peak at -17.4 eV. In the lower valence-band (VB) region (the O $2p$ bonding band from -5.2 to -10.7 eV), there is one prominent peak at -6.0 eV and a smaller peak at -7.5 eV. This is separated from the upper VB (the O $2p$ lone pair band from 0 to -4.7 eV) by a sizable gap of 0.5 eV. The presence of this gap in a-SiO_2 is attributed to the near perfectness of the CRN model in the present case. In other calculations where the models contain large BL and BA distortions or have under- or overcoordinated atoms, this gap is likely to disappear. The upper VB of

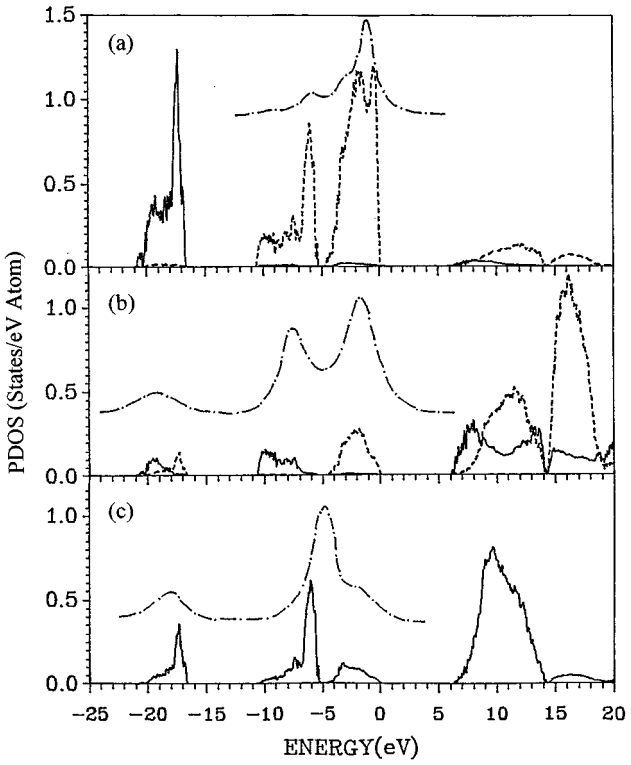

FIG. 6. Orbital resolved partial DOS of a-SiO_2: (a) O $2s$ (solid line) and O $2p$ (dashed line), (b) Si $3s$ (solid line) and Si $3d$ (dashed line), and (c) Si $3p$. The experimental x-ray emission data (dash-dotted line) for O K, Si K (Ref. 52), and Si $L_{2,3}$ (Ref. 53) in α quartz are also sketched.

a-SiO_2 has a main peak at -2.0 eV and a sharp leading peak at -0.3 eV. In c-SiO_2, both the upper and lower VB's have multiple peaks rooting from the van Hove singularities of the quartz structure. The conduction-band (CB) DOS of the two SiO_2 phases are also quite different. In a-SiO_2, there are two broadbands, one from 6.0 to 14.3 eV and another from 14.3 eV to 19.0 V. The CB of c-SiO_2 also has these two well-separated pieces, but they have many multiple-peak structures. The most significant difference is the curvature of the DOS at the lower CB edge. It is parabolic in c-SiO_2, where there is a single CB with a minimum at Γ,[42] but appears to be linear in the case of a-SiO_2. The calculated LDA gap for a-SiO_2 is 6.0 eV, a reduction of 0.65 eV from the c-SiO_2 gap of 6.65 eV.[50] This is in good agreement with the measurements of Appelton, Chiranjivi, and Jafaripour,[51] which shows a reduction of the gap of the order of 0.5 eV.

The orbital decompositions of the DOS for a-SiO_2 are shown in Fig. 6. It is shown that the Si $3d$ orbitals contribute significantly to the CB DOS, especially in the upper portion, and the states near the CB minimum are mostly Si $3s$ and $4s$ in character. On the same diagram we display the experimental O K, Si K, and Si $L_{2,3}$ x-ray emission spectra for α quartz.[52,53] We cannot locate similar data for a-SiO_2, but they are expected to be similar. In the simple approximation of localized core levels of the emitting atom, the O K, Si K, and Si $L_{2,3}$ x-ray emission spectra mimic, respectively, the O $2p$, Si $3p$, and Si $3s$ plus Si $3d$ partial DOS in the VB because of the dipole selection rules. The agreement with the calculated partial DOS for a-SiO_2 is quite good. In particu-

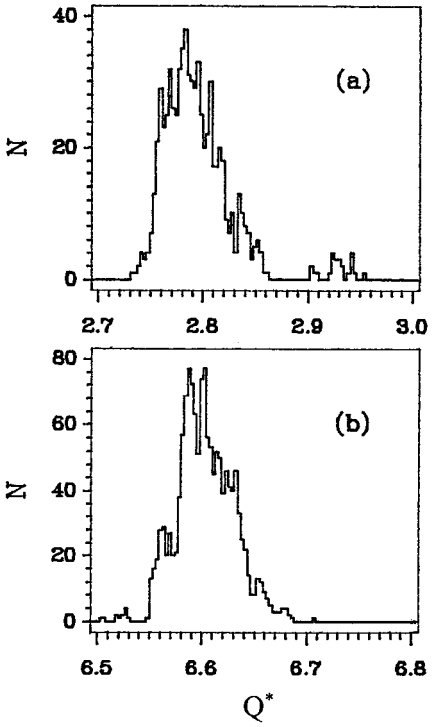

FIG. 7. Distribution of calculated effective charges: (a) Q^*_{Si} and (b) Q^*_O.

lar, the double peak in the Si $L_{2,3}$ spectrum in which the leading peak has a higher amplitude is fully explained. This is due to the fact the Si 3*d* has a significant component in the upper VB while the Si 3*s* component at the lower VB has its near peak skewed towards the lower energy near 10 eV.

B. Effective charges

Figure 7 shows the distributions of the calculated effective charges Q^*_{Si} for the 432 Si atoms and Q^*_O for the 864 O atoms. They are obtained from the wave functions and the overlap integrals $S_{i\alpha,j\beta}$ based on the Mulliken scheme:[54]

$$Q^*_\alpha = \sum_{n,\mathrm{occ}} \sum_i \sum_{j,\beta} C^n_{i,\alpha} C^n_{j,\beta} S_{i\alpha,j\beta}. \quad (1)$$

Here the summation over n is for the occupied levels. α,β label the atoms and i,j the orbitals and $C^n_{i\alpha}$ are the eigenvector coefficients. The average value for Q^*_{Si} is 2.79 electrons and that for Q^*_O is 6.66 electrons with standard deviations of 0.036 and 0.038 electron, respectively. Thus the partially ionic nature of bonding in a-SiO_2 glass is evident. It should be remembered that the effective charge calculation based on Mulliken's scheme is only approximate. A more accurate procedure based on real-space charge integration gives $Q^*_{Si}=1.40$ and $Q^*_O=7.30$ for a quartz.[42] With the exception of a few scattered points, the data for Q^*_{Si} and Q^*_O show a reasonable normal distribution. To answer a deeper question of how the effective charges are correlated with the BL and BA distributions in a-SiO_2, we plot in Fig. 8 the Q^*_{Si} and Q^*_O against the average BL associated with each atom. Also shown is a plot of Q^*_O against the Si-O-Si bridging angle. Comparing Fig. 8 with the BL and BA distributions of Fig. 2, it is quite clear that there is no obvious correlation of Q^*_{Si} with BL or Q^*_O and Q^*_{Si} with the bridging angle, but there appears to be a weak correlation between Q^*_O and the BL. Namely, O atoms with shorter Si-O BL tend to have a larger effective charge.

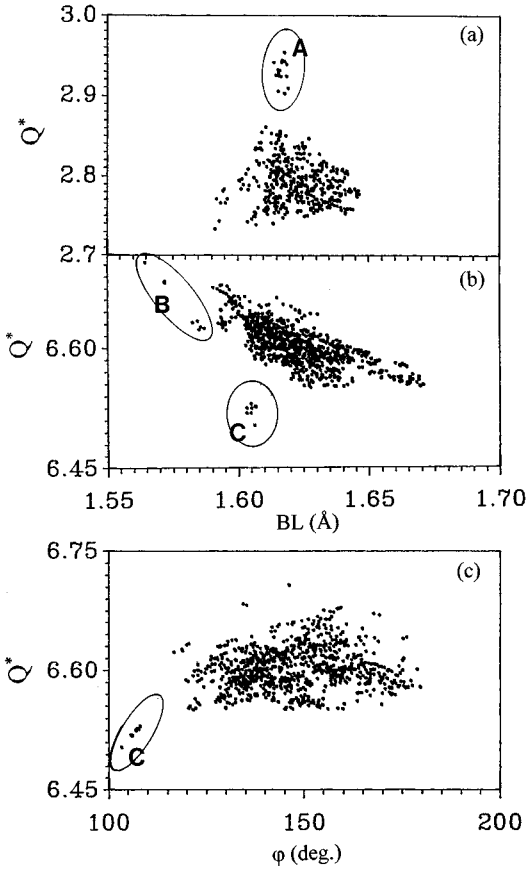

FIG. 8. Correlation plot of (a) Q^*_{Si} with Si-O BL, (b) Q^*_O with Si-O BL, and (c) Q^*_O with Si-O-Si angles. Groups of atoms *A*,*B*,*C* are circled.

C. Quasidefective O centers

A more conspicuous picture of Fig. 8 is the fact that there is a group of 16 Si atoms (designated as group *A*) with Q^*_{Si} above 2.90, a group of 8 O atoms (designated as group *B*) with Si-O BL less than 1.59 Å and Q^*_O above 6.62, and a group of 8 O atoms (designated as group *C*) with Q^*_O less than 6.53. By analyzing the local structure of these atoms in the network model, we found the following. (i) The group-*A* Si atoms are the NN's of group-*C* O atoms. The effective charges of these two groups indicate a reduced charge transfer from Si to O. (ii) The group-*C* atoms are the same O atoms with much smaller Si-O-Si bridging angles discussed in Fig. 2. They range from 103.35° to 107.63°. (iii) The BL's of the O-Si pair in groups *A* and *C* are within the normal range, about 1.62 Å. (iv) The deviation of the O-Si-O angles from the tetrahedral angle for Si atoms in group *A* are minimal, indicating rather rigid tetrahedral units. (v) The group-*B* O atoms have smaller BL, ranging from 1.56 to 1.59 Å, and also smaller Si-O-Si angles, ranging from 116.5° to 146.2°. Thus we see that within a reasonable range of distortion,

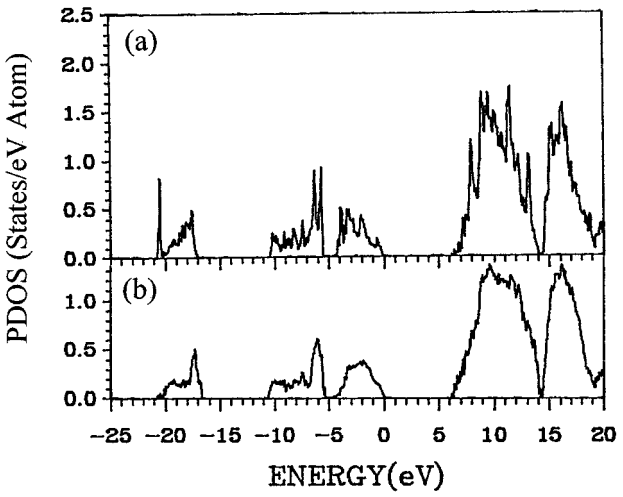

FIG. 9. Average local DOS of (a) Si atoms in group A and (b) Si atoms in bulk a-SiO_2.

there is no strong correlation of Q_O^* and Q_{Si}^* to the Si-O-Si angle and only a weak correlation of Q_O^* with the Si-O BL. However, when the Si-O-Si angle becomes too small, say, below 120°, the Q_O^* tends to decrease and the Q_{Si}^* of its NN Si tends to increase, resulting in a reduction in the ionicity of the network.

To further investigate the electronic structure of the group-A, -B, -C atoms, we calculate their local DOS (LDOS), which are shown in Figs. 9 and 10. Also shown for comparison are the LDOS for Si and O for the bulk a-SiO_2. Clearly, the Si LDOS are very similar to the LDOS of the other Si in the network except for the strong bonding peak

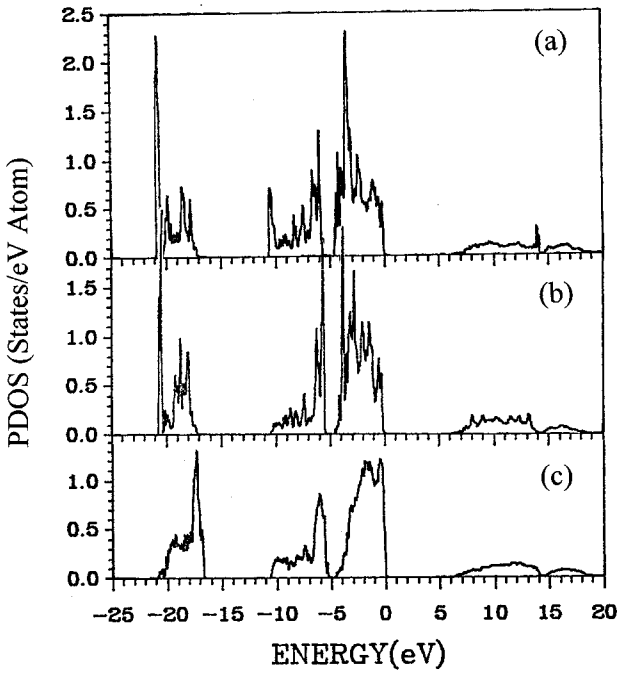

FIG. 10. Average local DOS of (a) O atoms in group B, (b) O atoms in group C, and (c) O atoms in bulk a-SiO_2.

with O 2s at −21 eV, but the LDOS of the O in group B and C differ from the bulk O significantly. The main features are the shifting of the centers of gravities of the DOS in all three bands, the O 2s band and the lower and the upper VB. Extra sharp peaks at −20.7, −10.4, and −3.4 eV (for O in group B) and at −20.5 and −3.8 eV (for O in group C) are introduced. All these indicate an increase in the interaction energy due to reduction in the Si-O-Si bridging angle and a concomitant reduction in the Si-Si separation between the two adjacent tetrahedron units. More concisely, we may regard these O atoms with small bridging angles as quasidefective centers in a-SiO_2 and there are certainly many of them in a real glass. It has been demonstrated in a number of experiments[55–59] that the densification of a-SiO_2 glass under pressure leads to the reduction in the Si-O-Si angle. These quasidefective centers can be the microscopic origin of the two-level tunneling that is responsible for the experimentally observed linear specific heat behavior at low temperature in a-SiO_2 and many other ionic glasses.[60] We will return to the discussion of this point in Sec. IV.

D. Localization of band-edge states

An important quantity in the analysis of electron states of a noncrystalline solid is its degree of localization. It is well known that the states near the band edges are localized and those in the center of the band are delocalized.[61] However, it can also happen that the states in the middle of the band can be localized depending on the potential, the nature of the interaction, as well as how a band is defined. As will be shown later, there can be states relatively localized even though they are not at the edges of what appears to be a continuous distribution of states with no gaps. In the present analysis of localization, realistic wave functions are used, in contrast to those obtained from model studies with some rather severe approximations.[62] Because the system we study is a finite one, the degree of localization we discuss with our results is a relative one and cannot or should not be interpreted in the formal sense that is appropriate only for an infinite system.

For each state n, we can characterize it by a localization index L_n, which in the OLCAO formalism takes the form

$$L_n = \sum_{i,\alpha} \left[\sum_{j,\beta} C_{i,\alpha}^n C_{j,\beta}^n S_{i\alpha,j\beta} \right]^2 . \tag{2}$$

Such a characterization of the wave function localization is meaningful if and only if the model for the noncrystalline solid is sufficiently large. The difference between a localized and an extended state in any finite calculation of N atoms is only relative since for a truly extended state, L_n should be 0, which can only be attained in the limit of $N \to \infty$. Figure 11(a) shows the calculated L_n of all the states in the a-SiO_2 model across the entire energy range, which should be studied together with the DOS diagram of Fig. 5(b). The result is very striking, showing clearly the localization of the states near the band edges. A similar analysis was carried out by Ching with a much smaller model of only 162 atoms.[43] It is interesting to find some relatively localized states at around −6.5 eV well within the lower VB. This implies that the sharp peak at −6.0 eV in Fig. 5(b) should be considered as a single

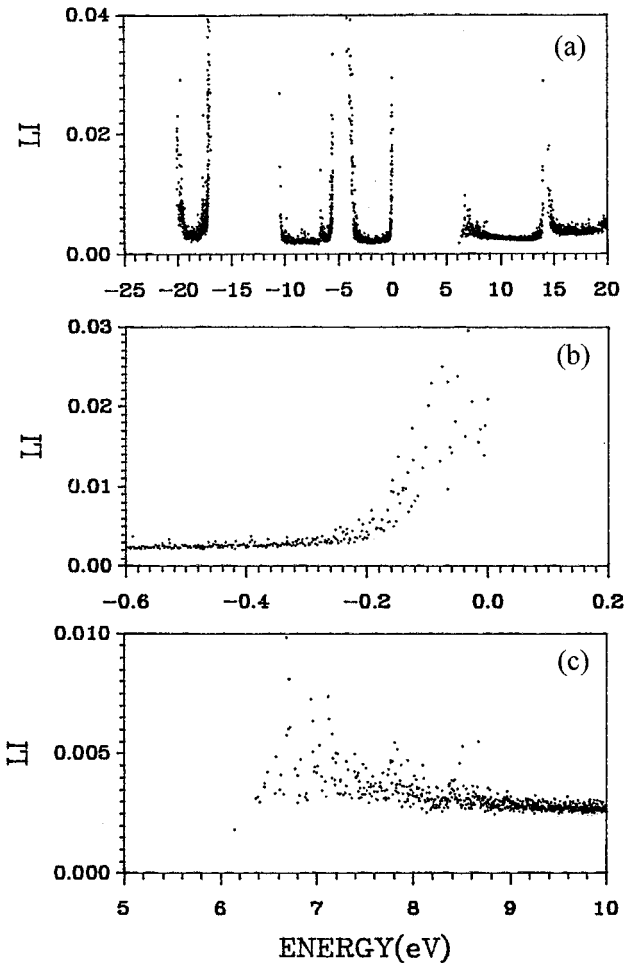

FIG. 11. Localization index of the electron states in a-SiO_2 (a) for the entire range of states, (b) for states at the top of the VB, and (c) for states at the edge of the CB.

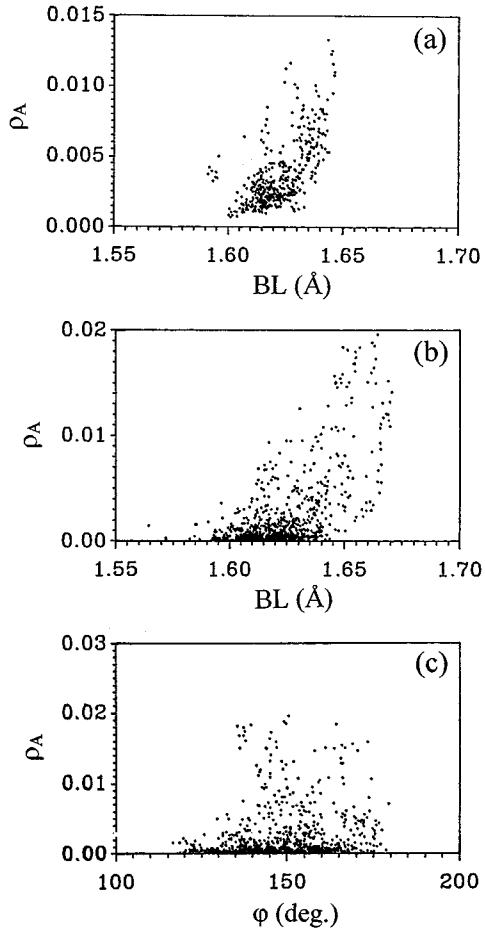

FIG. 12. Correlation of ρ_A with the Si-O BL (a) for states on Si near the bottom of the CB, and (b) for localized states on O at the top of the VB. (c) Correlation of ρ_A with the Si-O-Si angle for states on O atoms at the top of the VB.

band by itself and the localized states near -6.5 eV are the lower band-edge states of this particular band. Thus, as far as the electron states in a non-crystalline solid are concerned, a more appropriate definition for a band should be the existence of localized states at the band edges, not necessarily by the existence of a well-defined gap.

The localized states near the top of the VB and the bottom of the CB are particularly important. It has been long established that at these edges, localized and extended states are separated by a mobility edge, which is an intrinsic property of a non-crystalline semiconductor or insulator.[62] In a finite calculation, the location of this mobility edge can only be approximate. Nevertheless, a good estimation is possible with calculations on a large model. In Figs. 11(b) and 11(c), we plot the L_n of the states near the VB and the CB edges in the expanded scale. A mobility edge of approximately 0.2 eV in the VB can be estimated. This value can be considered as an upper bond since the estimated mobility edge may be somewhat size dependent. In the CB edge, the localization of states is less obvious because of the more extended nature of the unoccupied antibonding states and a mobility edge cannot be assigned. Ching had pointed out[43] that this can explain the experimental observation of high mobility of injected electrons in a-SiO_2.[63]

It is instructive to see on which atoms the localized states at the band edges localize. To this end, we analyze their wave functions. Since a large L_n is obtained from large fractional charges, which are the projections of the wave function on the basis orbitals centered on these atoms, we average the fractional charges over about 20 localized states at each of the band edge and obtain a value we call ρ_A for each atom. We then attempt to correlate ρ_A with the BL and BA associated with these atoms. The results are shown in Fig. 12. Because states at the top of the VB are exclusively derived from the O orbitals and at the bottom of the CB are dominated by the Si orbitals, the correlation study is for ρ_A with the Si-O BL and the Si-O-Si angle for the localized states at the top of the VB and for the ρ_A with the Si-O bond for the relatively localized states at the bottom of the CB. It can be seen from Fig. 12 that in the both cases, localization of states is induced by the elongation of the Si-O bond with no clear correlation to the Si-O-Si angle. This is quite understandable since the bridging angles in a-SiO_2 glass are very flexible and should not affect the degree of localization that much. On the other hand, elongation of the bond tends to localize the charges to the atoms of that bond. Figures 13(a) and 13(b) show the correlation of ρ_A to BL for states at the

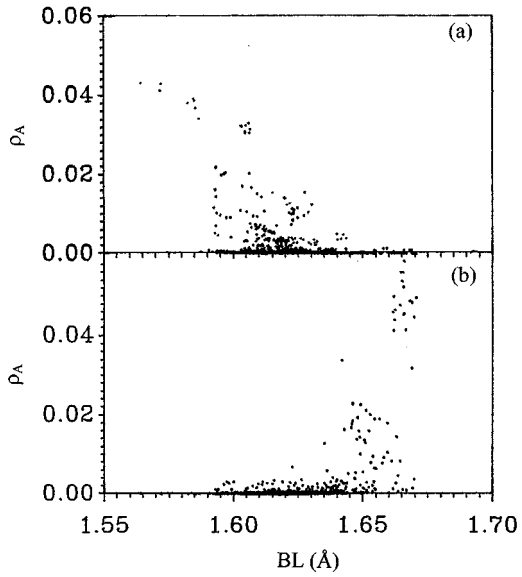

FIG. 13. Correlation of ρ_A (defined in the text) with BL for states at the (a) bottom of the O 2s band and (b) top of the O 2s band.

bottom and the top of the O 2s band. Similar results are obtained at the other regions of the VB. It is clear that in the occupied region, the localization of the wave function at the bottom of a given band is induced by the contraction of the bond, while that at the top of the band is induced by the elongation of the bond, as already shown for the top of the VB. Obviously, bond contraction results in the increased overlap between the atoms and hence a lowering in the binding energy, which then should occur at the bottom of the band.

IV. DISCUSSION

Based on the first-principles calculation of the electronic structure of a large and near-perfect CRN model for a-SiO_2, many insights about the electron states in such a noncrystalline solid are obtained. First, it is shown that the DOS of c-SiO_2 and a-SiO_2 have subtle differences reflecting the different LRO and IRO in these two phases. Experimental probes such as x-ray photoemission experiments are not of sufficient high resolution to distinguish these two phases. Traditionally, it has been taken for granted that the electronic structures of c-SiO_2 and a-SiO_2 are essentially the same because of the similarity in the local bonding structure. Second, the electronic-structure results are correlated with the structural characteristics of the model. In a noncrystalline solid, the structural parameters such as BL and BA distributions are the physical parameters of the solid. It is demonstrated that some correlation exists between the effective charges of O with the Si-O bond length, but much less for the effective charges of Si. The same is true for the qualitative estimation of the degree of localization of the wave functions at the band edges. It is also shown that O atoms with small bridging angles can be regarded as quasidefective centers, which show significant deviation of their local DOS and the effective charges from that of bulk O atoms in a-SiO_2. Because of the large size of the model, it is possible to make a reliable estimation for the mobility edge at the top of the VB in a-SiO_2. It is also shown that a similar estimation of the mobility edge for the CB may not be possible because of the relatively delocalized nature of the CB wave functions.

One of the outstanding problems of the physics of glasses is the identification of the two-level tunneling centers in covalent glasses,[60] which give rise to the linear specific heat and anomalies in the heat capacity measurements.[64–66] It has been argued that such experimental phenomena can be accounted for by the tunneling mechanism between two nearly equivalent configurations of atoms or groups of atoms corresponding to the minima of an asymmetric double potential well.[67] Many theories have been put forth to account for such tunneling centers.[67–72] However, the microscopic origin of these tunneling centers is still a matter of controversy.[60] We would like to argue that the O atoms with smaller than usual Si-O-Si angles discussed above are the likely candidates for these tunneling centers based on the following observations. (i) Such O centers are very likely to exist in the quenching process and their number density cannot be too high because of the overall steric hindrance of the CRN structure. Also, such centers can exist in other oxide or chalcogenide glasses, thus establishing the universal nature of these tunneling centers.[60,73] (ii) An electronic-structure calculation shows these O atoms to be quasidefective with different effective charges and LDOS. However, because no broken bonds are introduced and no over- or undercoordination of atoms are envisioned, the energy separations of these centers are expected to be small, much smaller than, say, the introduction of defects or impurities. As far as the low-frequency vibrational modes are concerned, these centers should have very close energies for tunneling to be operative. The distribution of the energy splitting Δ of two such configurations can be quite small, and is related to the topological structure of the random network, and is expected to be flat on the scale of the thermal energy kT. (iii) Tunneling can be described as the rearrangement of these quasidefective O atoms. Namely, an O atom with a small Si-O-Si angle can move to increase the bridging angle but simultaneously reduce the bridging angle of a nearby O atom. This is similar to the coupled rotation of the tetrahedra linked at the O center that supports the soft mode vibration.[74,75] (iv) The existence of the small Si-O-Si angles in a-SiO_2 need not be associated with the existence of three- or four-members rings in the network as suggested by Galeener *et al.*[27] It has been shown earlier by Murray and Ching[24] that the so-called $D1$ and $D2$ centers in the vibrational spectrum can be explained by the existence of the O centers with smaller than usual Si-O-Si angles. This proposal relating small bridging angle O atoms to the two-level tunneling centers can be further tested by detailed calculation on the vibrational DOS of the model.

A large near-perfect CRN model for the type studied here is extremely valuable since it can be the basis of generating other network models with solutes, network modifiers, interstitial or substitutional defects, etc., under strictly controlled conditions. The present study certainly can be extended to other types of CRN models of glasses with different local bonding patterns such as in a-B_2O_3 or a-Si_3N_4. The strategy of large-scale structure modeling followed by the calculation

of electron states can be applied to the study of composite mixtures of these glasses or microcrystalline inclusion in a glass matrix. For example, the amorphous mixtures of a-Si and a-SiO_2 were studied before along this line in the context of either a random bond model or a random mixture model.[49] While these earlier calculations were based on rather small models and the conclusions reached were less definitive, the enlarged models of the present type can bring insights into the understanding of electron states in noncrystalline covalent glasses and their interfaces. It is also possible to use the wave functions obtained to calculate other physical properties such as the dielectric properties of these highly complex systems and compare with the experimentally measured data from vacuum ultraviolet optical absorption measurements or electron energy-loss spectroscopy. In this respect, structural modeling followed by first-principles calculations can be a very effective probe in understanding the nature of electron states in the highly complex multicomponent mixtures and glasses.

ACKNOWLEDGMENTS

This work was supported by the Department of Energy under Grant No. DE-FG02-84ER45170 and in part by the University of Missouri Research Board. We also acknowledge the assistance of Honyu Yao in the model construction.

[1] F. L. Galeener, in *The Physics and Technology of Amorphous SiO_2*, edited by R. A. B. Devine (Plenum, New York, 1987), p. 1.
[2] W. H. Zachariasen, J. Am. Chem. Soc. **54**, 3841 (1932).
[3] B. E. Warren, J. Appl. Phys. **8**, 645 (1937).
[4] D. L. Evans and S. V. King, Nature **212**, 1353 (1966).
[5] R. J. Bell and P. Dean, Philos. Mag. **25**, 1381 (1972).
[6] P. H. Gaskell and I. D. Tarrant, Philos. Mag. B **42**, 265 (1980).
[7] W. Y. Ching, Phys. Rev. B **26**, 6610 (1982).
[8] T. F. Soules, J. Non-Cryst. Solids **49**, 29 (1982).
[9] S. K. Mitra, Philos. Mag. B **45**, 529 (1982).
[10] S. H. Garofalini, J. Chem. Phys. **76**, 3189 (1982).
[11] F. L. Galeener, Philos. Mag. B **51**, L1 (1985).
[12] Y. T. Thathachari and W. A. Tiller, J. Appl. Phys. **57**, 1805 (1985).
[13] L. F. Gladden, T. A. Carpenter, and S. R. Elliott, Philos. Mag. B **53**, L81 (1986).
[14] N. Rivier, Adv. Phys. **36**, 95 (1987).
[15] B. P. Feuston and S. H. Garofalini, J. Chem. Phys. **89**, 5818 (1988).
[16] L. Guttman and S. M. Rahman, Phys. Rev. B **37**, 2657 (1988).
[17] C. S. Marians and L. W. Hobbs, J. Non-Cryst. Solids **124**, 242 (1990).
[18] P. Vashishta, R. K. Kalia, J. P. Rino, and I. Ebbsjö, Phys. Rev. B **41**, 12 197 (1990).
[19] L. F. Gladden, J. Non-Cryst. Solids **119**, 318 (1990).
[20] S. L. Chan and S. R. Elliott, Phys. Rev. B **43**, 4423 (1991).
[21] L. Stixrude and M. S. T. Bukowinski, Phys. Rev. B **44**, 2523 (1991).
[22] W. Y. Ching, Phys. Rev. B **26**, 6622 (1982).
[23] R. P. Gupta, Phys. Rev. B **32**, 8287 (1985).
[24] R. A. Murray and W. Y. Ching, Phys. Rev. B **39**, 1321 (1989).
[25] J. Sarnthein, A. Pasquarello, and R. Car, Phys. Rev. Lett. **74**, 4682 (1995).
[26] R. J. Bell, N. F. Bird, and P. Dean, J. Phys. C **1**, 299 (1968).
[27] F. L. Galeener, R. A. Barrio, E. Martinez, and R. J. Elliott, Phys. Rev. Lett. **53**, 2429 (1984).
[28] L. Guttman and S. M. Rahman, J. Non-Cryst. Solids **75**, 419 (1985).
[29] F. L. Galeener and A. C. Wright, Solid State Commun. **57**, 677 (1987).
[30] R. L. Mozzi and B. E. Warren, J. Appl. Crystallogr. **2**, 164 (1969).
[31] J. H. Konnert and J. Karle, Acta Crystallogr. Sec. A **29**, 702 (1973).
[32] M. Misawa, D. L. Price, and K. Suzuki, J. Non-Cryst. Solids **37**, 85 (1980).
[33] F. L. Galeener, A. J. Leadbetter, and M. W. Stringfellow, Phys. Rev. B **27**, 1052 (1983).
[34] A. C. Wright and R. N. Sinclair, J. Non-Cryst. Solids **76**, 351 (1985).
[35] Y. Tanaka, N. Ohtomo, and M. Katayama, J. Phys. Soc. Jpn. **54**, 967 (1985).
[36] J. M. Carpenter and D. L. Price, Phys. Rev. Lett. **54**, 441 (1985).
[37] U. Buchenau, N. Nucker, and A. J. Dianoux, Phys. Rev. B **34**, 5665 (1986).
[38] U. Water, D. L. Price, S. Susman, and K. J. Volin, Phys. Rev. B **37**, 4232 (1988).
[39] M. Arai, D. L. Price, S. Susman, K. J. Volin, and U. Walter, Phys. Rev. B **37**, 4240 (1988).
[40] A. C. Wright, J. Non-Cryst. Solids **106**, 1 (1988).
[41] S. Susman, K. J. Volin, D. L. Price, M. Grimsditch, J. P. Rino, R. K. Kalia, P. Vashishta, G. Gwanmesia, Y. Wang, and R. C. Liebermann, Phys. Rev. B **43**, 1194 (1991).
[42] Y.-N. Xu and W. Y. Ching, Phys. Rev. B **44**, 11 048 (1991).
[43] W. Y. Ching, Phys. Rev. Lett. **46**, 607 (1981).
[44] P. Keating, Phys. Rev. **145**, 637 (1966).
[45] R. Dupree and R. F. Pettifer, Nature **308**, 523 (1984).
[46] Y. Waseda, *The Structures of Non-Crystalline Materials* (McGraw-Hill, New York, 1980).
[47] W. Y. Ching, J. Am. Ceram. Soc. **71**, 3135 (1990).
[48] Y. P. Li and W. Y. Ching, Phys. Rev. B **31**, 3172 (1985).
[49] W. Y. Ching, Phys. Rev. B **26**, 6633 (1982).
[50] The calculated LDA band gap for α quartz using a full basis set in Ref. 42 is 5.80 eV. A LDA gap of 6.65 eV is obtained by excluding the O 3s and O 3p orbitals in the basis set. Other than the LDA gap, no discernible differences in the calculated DOS are found.
[51] A. A. Appleton, T. Chiranjivi, and M. Jafaripour, in *Physics of SiO_2 and Its Interfaces*, edited by S. T. Pantelides (Pergamon, New York, 1978).
[52] G. Wiech, E. Zopf, H. U. Chun, and R. Bruckner, J. Non-Cryst. Solids **21**, 251 (1976).
[53] G. Wiech, Solid State Commun. **52**, 807 (1984).
[54] R. S. Mulliken, J. Chem. Phys. **23**, 1833 (1955).
[55] R. J. Hemley, K. Mao, P. M. Bell, and B. O. Mysen, Phys. Rev. Lett. **57**, 747 (1986).
[56] R. A. B. Devine and J. Arndt, Phys. Rev. B **35**, 9376 (1987); **39**, 5132 (1989).

[57] Q. Williams and R. Jeanloz, Science **239**, 902 (1988).
[58] L. Stixrude and M. S. T. Bukowinski, Phys. Rev. B **44**, 2523 (1991).
[59] N. Kitamura, K. Fuikumi, K. Kandono, H. Yamashita, and K. Suito, Phys. Rev. B **50**, 132 (1994).
[60] W. A. Phillips, Rep. Prog. Phys. **50**, 1657 (1987).
[61] M. H. Cohen, J. Signh, and F. Yonezawa, Solid State Commun. **36**, 923 (1980).
[62] S. Kirkpatrick and T. P. Eggarter, Phys. Rev. B **6**, 3598 (1972).
[63] See, for example, N. F. Mott and E. A. Davis, *Electronic Processes in Non-Crystalline Materials*, 2nd ed. (Clarendon, Oxford, 1979).
[64] R. C. Hughs, Appl. Phys. Lett. **26**, 436 (1975).
[65] R. B. Stephens, Phys. Rev. B **13**, 852 (1976).
[66] M. P. Zaitlin and A. C. Anderson, Phys. Rev. B **12**, 4475 (1975).
[67] U. Buchenau, N. Nucker, and A. J. Dianoux, Phys. Rev. Lett. **53**, 2316 (1984).
[68] P. W. Anderson, B. I. Halperin, and C. M. Varma, Philos. Mag. **25**, 1 (1972).
[69] K. K. Mon and N. W. Aschroft, Solid State Commun. **27**, 609 (1977).
[70] M. H. Cohen and G. S. Grest, Phys. Rev. Lett. **45**, 1271 (1980).
[71] J. C. Phillips, Phys. Rev. B **24**, 1744 (1981).
[72] M. F. Thorpe, J. Non-Cryst. Solids **57**, 355 (1983).
[73] C. C. Yu and J. J. Freeman, Phys. Rev. B **36**, 7620 (1987).
[74] S. A. Fitzgerald, J. A. Campbell, and A. J. Sievers, Phys. Rev. Lett. **73**, 3105 (1994).
[75] C. Laermans and V. Keppens, Phys. Rev. B **51**, 8158 (1995).